

Quantification of Amyloid Deposition in Alzheimer's Disease Patients Using PET and [11C]BF-227

著者	Tashiro M., Okamura N., Watanuki S., Furumoto S., Furukawa K., Funaki Y., Iwata R., Kudo Y., Arai H., Watabe H., Yanai K.
journal or publication title	CYRIC annual report
volume	2009
page range	164-170
year	2009
URL	http://hdl.handle.net/10097/50507

VIII. 6. Quantification of Amyloid β Deposition in Alzheimer's Disease Patients Using PET and [^{11}C]BF-227

Tashiro M.¹, Okamura N.³, Watanuki S.¹, Furumoto S.^{2,3}, Furukawa K.⁴, Funaki Y.²,
Iwata R.², Kudo Y.⁵, Arai H.⁴, Watabe H.⁶, and Yanai K.^{1,2}

¹Divisions of Cyclotron Nuclear Medicine and ²Radiopharmaceutical Chemistry,
Cyclotron and Radioisotope Center, Tohoku University

³Department of Pharmacology, Tohoku University Graduate School of Medicine

⁴Department of Geriatrics and Gerontology, Institute of Development, Aging and Cancer, Tohoku University

⁵Innovation of New Biomedical Engineering Center, Tohoku University

⁶Department of Molecular Imaging in Medicine, Osaka University Graduate School of Medicine

Introduction

In Japan, incidence of cognitive disorders has been increasing and clinical studies on dementia have been very important. Functional neuroimaging of early Alzheimer's disease (AD) using PET and [^{18}F]fluorodeoxyglucose ([^{18}F]FDG) has demonstrated that a decrease in the cerebral metabolic rate of glucose (CMR_{glc}) often starts in the posterior cingulate gyrus and further propagates to the temporo-parietal regions and others. But the regional metabolic reduction is not so obvious and widespread in the early stage of disease course including mild cognitive impairment (MCI)¹. Neuronal damage is associated with high deposition of amyloid β ($\text{A}\beta$) protein in the brain, and massive neuronal loss is often preceded by high $\text{A}\beta$ deposition. An early diagnosis of mild AD can be established if we use a proper tracer that specifically-binds to $\text{A}\beta$ proteins in the brain of patients.

" $\text{A}\beta$ imaging" using PET has been recognized as one of the most important methods for diagnosing early AD partly because of excellent sensitivity of PET technique². A large number of candidate compounds have already been tested in basic studies and several compounds were selected for clinical studies³. Clinical PET studies have been conducted using several probes such as [^{18}F]FDDNP⁴), [^{11}C]SB-13⁵) and [^{11}C]Pittsburgh compound-B ([^{11}C]PIB)⁶, among which [^{11}C]PIB has been used the most widely in the world⁶⁻⁸). Many studies have clearly demonstrated that the [^{11}C]PIB binds to $\text{A}\beta$ fibrils, enabling noninvasive assessment of $\text{A}\beta$ deposition in the brain of AD patients as a biomarker for AD⁶.

Considering the importance of A β imaging, our group also developed a novel PET tracer, 2-(2-[2-demethylaminothiazol-5-yl]ethenyl)-6-(2-[fluoro]ethoxy)benzoxazole (BF-227), probably the first original compound used for human study in Japan⁹. Our clinical study has demonstrated that this compound is able to finely detect A β deposition primarily in the posterior association area of AD patients and accumulation in the frontal area is not prominent. In contrast to [¹¹C]PIB, interestingly, [¹¹C]BF-227 seems to be able to detect senile plaques containing dense amyloid fibrils preferentially, providing unique and specific information regarding the A β pathology in AD patients⁹. In addition, we compared the [¹¹C]BF-227 PET to structural MRI and FDG PET for diagnosing and tracking the severity of AD, to demonstrate that [¹¹C]BF-227 PET was more sensitive than MRI in diagnosing AD and detecting converters from MCI to AD¹⁰. These studies have indicated that [¹¹C]BF-227 PET is a useful method for early diagnosis of AD and for predicting potential converters from MCI to AD^{10,11}.

Though these above PET studies have succeeded in demonstrating [¹¹C]BF-227 is a useful tracer, they have used standardized uptake values (SUV) as a tool for clinical evaluation, that is a semi-quantitative measure, simply corrected for the injected dose and the body size of the subject. Precise quantitative examination may give a better rationale to the use of such a simple method as a clinical tool, as experienced with [¹¹C]PIB^{7,8}. However, we have not conducted the precise examination of pharmacokinetics of [¹¹C]BF-227 in the human brain using arterial sampling data. In this paper, quantification methods for A β imaging with PET is briefly overviewed and preliminary results of [¹¹C]BF-227 PET are discussed.

Materials and Methods

For the present study, 6 AD patients (mean age: 73 years old) and 6 healthy volunteers (mean age: 61 years old) were recruited. PET scan was initiated simultaneously to the [¹¹C]BF-227 injection, in order to obtain dynamic data of 23 time frames. Serial arterial blood sampling was also done. Metabolite fraction was also examined using the blood data at 5, 15, 30 and 60 min post-injection and the fraction data were used for correction of input functions. The dynamic PET data were coregistered to the individual MRI T1 images for defining regions of interest (ROIs) in the cortex and subcortical deep nuclei (Figs. 1a and 1b). This study was approved by the ethics committee of Tohoku University Graduate School of Medicine, and informed consent was obtained from each

subject. In analysis, distribution volume (DV) and binding potential (BP) values of [¹¹C]BF-227 were estimated based on full kinetic compartmental model based on the 1-tissue (1TM) and 2-tissues models (2TM) (Fig. 1d). Graphical analysis methods were also applied using 2 types of Logan graphical analysis methods; one using the time-activity curve (TAC) of arterial plasma data as an input function for analysis (LGA)¹²⁾ and the other using the TAC of the reference brain tissue (cerebellum) (LGAR)¹³⁾ (Fig. 1c). PMOD software ver. 3.0 (PMOD Technologies, Zurich, Switzerland) was used for calculation. The results of compartmental model analysis and graphical analysis were compared to the SUV and the SUV ratios to the cerebellar SUV (cerebellar SUVR). Correlations among these different methods were examined one another¹⁴⁾.

Results

No clear difference was observed in the plasma TAC between AD patients and controls. But, clear difference was observed in the tissue TAC between AD patients and controls. [¹¹C]BF-227 accumulation was significantly higher in the cerebral cortex than in the cerebellum of AD patients, while there was no difference in Control. In the analysis results, it turned out that 2TM better described the pharmacokinetics of [¹¹C]BF-227 than 1TM (Fig. 2). The DV and BP values of [¹¹C]BF-227 showed significantly higher in AD patients than in controls, and the most prominent difference was observed in the temporo-occipital and lateral temporal regions¹⁴⁾. Next, both the DV values correlated well between the two methods such as 2TM and LGA ($r^2 > 0.95$ in all regions). In addition, results of LGA and LGAR also correlated well. The LGA values also correlated well to the SUV and SUVR ($r^2 > 0.94$ in all regions)¹⁴⁾.

Discussion

Nowadays, A β imaging using PET has been recognized as one of the most effective methods for diagnosing early AD and for predicting potential converters from MCI to AD^{2,6)}. Several promising⁵⁾ and [¹¹C]PIB⁶⁾, among which [¹¹C]PIB has been regarded as the most successful A β imaging probe. Though an initial study was done without arterial blood sampling and mainly used SUV for clinical evaluation⁶⁾, the results of quantitative study was reported in the details⁸⁾.

Initial studies using [¹¹C]BF-227 have been conducted in a similar manner. Kudo and colleagues reported that this compound was able to finely detect A β deposition

primarily in the posterior association area of AD patients, suggesting that [^{11}C]BF-227 might be able to detect senile plaques containing dense amyloid fibrils preferentially, in contrast to [^{11}C]PIB, providing unique and specific information regarding the A β pathology in AD patients⁹). In addition, we performed the comparative study between [^{11}C]BF-227 PET and structural MRI for the diagnosis and tracking the severity of AD. The results demonstrated that PET and [^{11}C]BF-227 was more sensitive than the result of MRI voxel-based morphometry (VBM)¹⁰. Another study demonstrated that [^{11}C]BF-227 was more sensitive than FDG PET in diagnosing AD and detecting converters from MCI to AD¹¹). Thus, these studies may suggest that A β PET imaging is more sensitive than the detection of hippocampal atrophy using MRI and the glucose metabolic reduction measured by PET, in diagnosing early AD and predicting potential converters from MCI to AD.

The pharmacokinetics of [^{11}C]PIB has been thoroughly examined using various quantification methods such as full kinetic analysis and graphical analysis^{7,8}). In their full kinetic analyses, commonly-used compartmental models are the 3 compartmental model (2-tissue compartmental model: 2TM), where one blood compartment and 2 tissue compartments with specific and non-specific binding are assumed, and the 2 compartmental model (1-tissue compartmental model: 1TM), where one tissue compartment represents both the specific and non-specific binding^{7,8}). When the tracer penetrates the blood-brain barrier (BBB) into the tissue compartment very rapidly, 1-tissue compartmental model might better describe the kinetics of the tracer. In the analysis of [^{11}C]PIB, it seems that the 2TM better described the kinetics of tracer binding to the A β in the human brain^{7,8}). Price and colleagues reported that Logan graphical analysis (LGA) were more useful and robust than the result of analysis using 2TM. However, interesting point is that the cerebellum itself, the reference regions that is thought to be free of mature A β plaques, was better described based on the 2TM⁸). Though many [^{11}C]PIB papers employ the use of DVR values for clinical evaluation, the use of BP was also proposed in the paper by Mintun and colleagues⁷).

As for [^{11}C]BF-227, the results of compartmental analysis indicated that 2TM showed better fitting than 1TM likely in the case of [^{11}C]PIB⁸). Linearization by LGA method was also successful, likely in the case of [^{11}C]PIB. Significant correlation between the DV values calculated by 2TM and LGA (and LGAR, as well) may suggest that Logan methods are fully applicable to the quantification of [^{11}C]BF-227. Significant correlation of the results of Logan methods to the SUV (and SUVR) may suggest that clinical evaluation

of A β deposition using [¹¹C]BF-227 PET can be done by using LGA (and LGAR, as well) and SUV and SUVR. These results can reconfirm the reliability of the results of our recent studies⁹⁻¹¹⁾.

In summary, it is demonstrated that [¹¹C]BF-227 is a promising tracer for A β imaging; diagnosing AD patients and detecting potential converters from MCI to AD. In addition to the study on AD diagnosis, recently, further clinical applications of [¹¹C]BF-227 PET have been tried and successful, for instance, to visualize pathological prion protein in prion diseases¹⁵⁾ and to imaging of α -synuclein deposition in multiple system atrophy¹⁶⁾.

For future prospects, in order to obtain more accurate examination, however, correction for partial volume effect should be considered. This partial volume correction (PVC) is important because of the following 2 reasons; one due to local atrophy in AD patients, and the other reason due to relatively high accumulation of [¹¹C]BF-227 in the white matter, as experienced in the analysis of [¹¹C]PIB PET⁸⁾.

Acknowledgments

This study was partly supported the grant-in-aids from the Ministry of Health, Welfare and Labor for Amyloid imaging, JST grant for education and research for molecular imaging. The authors thank to all the staffs of Cyclotron and Radioisotope Center, Tohoku University, for the operation of cyclotron and patients care.

References

- 1) Minoshima S., Foster N.L., Kuhl D.E., *Lancet* **344** (1994) 895.
- 2) Nordberg A., *Lancet Neurol.* **3** (2004) 519.
- 3) Furumoto S., Okamura N., Iwata R., Yanai K., Arai H., Kudo Y., *Curr. Top. Med. Chem.* **7** (2007) 1773.
- 4) Shoghi-Jadid K., Small G.W., Agdeppa E.D., Kepe V., Ercoli L.M., Siddarth P., Read S., Satyamurthy N., Petric A., Huang S.C., Barrio J. R., *Am. J. Geriatr. Psychiatry* **10** (2002) 24.
- 5) Verhoeff N.P., Wilson A.A., Takeshita S., Trop L., Hussey D., Singh K., Kung H.F., Kung M.P., Houle S. *Am. J. Geriatr. Psychiatry* **12** (2004) 584.
- 6) Klunk W.E., Engler H., Nordberg A., Wang Y., Blomqvist G., Holt D.P., Bergstrom M., Savitcheva I., Huang G.F., Estrada S., Ausen B., Debnath M.L., Barletta J., Price J.C., Sandell J., Lopresti B.J., Wall A., Koivisto P., Antoni G., Mathis C.A., Langstrom B., *Ann. Neurol.* **55** (2004) 306.
- 7) Mintun M.A., *CNS Spectr.* **10** (2005) 13.
- 8) Price J.C., Klunk W.E., Lopresti B.J., Lu X., Hoge J.A., Ziolkko S.K., Holt D.P., Meltzer C.C., DeKosky S.T., Mathis C.A., *J. Cereb. Blood Flow Metab.* **25** (2005) 1528.
- 9) Kudo Y., Okamura N., Furumoto S., Tashiro M., Furukawa K., Maruyama M., Itoh M., Iwata R., Yanai K., Arai H., *J. Nucl. Med.* **48** (2007) 553.
- 10) Waragai M., Okamura N., Furukawa K., Tashiro M., Furumoto S., Funaki Y., Kato M., Iwata R., Yanai K., Kudo Y., Arai H., *J. Neurol. Sci.* **285** (2009) 100.
- 11) Furukawa K., Okamura N., Tashiro M., Waragai M., Furumoto S., Iwata R., Yanai K., Kudo Y.,

- Arai H., *J. Neurol.* **257** (2010) 721.
- 12) Logan J., Fowler J.S., Volkow N.D., Wang G.J., Ding Y.S., Alexoff D.L., *J. Cereb. Blood Flow Metab.* **16** (1996) 834.
 - 13) Logan J., Fowler J.S., Volkow N.D., Wolf A.P., Dewey S.L., Schlyer D.J., MacGregor R.R., Hitzemann R., Bendriem B., Gatley S.J., et al., *J. Cereb. Blood Flow Metab.* **10** (1990) 740.
 - 14) Tashiro M., Okamura N., Watanuki S., Furumoto S., Furukawa K., Funaki Y., Iwata R., Kudo Y., Arai H., Watabe H., Yanai K., Quantitative Analysis of Amyloid β Deposition in Patients with Alzheimer's Disease Using Positron Emission Tomography. IN: *Early Detection and Rehabilitation Technologies for Dementia: Neuroscience and Biomedical Applications*, Editor: WU JINGLONG. Publisher: IGI Global. Philadelphia, USA (in press).
 - 15) Okamura N., Shiga Y., Furumoto S., Tashiro M., Tsuboi Y., Furukawa K., Yanai K., Iwata R., Arai H., Kudo Y., Itoyama Y., Doh-ura K., *Eur. J. Nucl. Med. Mol. Imaging* **37** (2010) 934.
 - 16) Kikuchi A., Takeda A., Okamura N., Tashiro M., Hasegawa T., Furumoto S., Kobayashi M., Sugeno N., Baba T., Miki Y., Mori F., Wakabayashi K., Funaki Y., Iwata R., Takahashi S., Fukuda H., Arai H., Kudo Y., Yanai K., Itoyama Y., *Brain* **133** (2010) 1772.

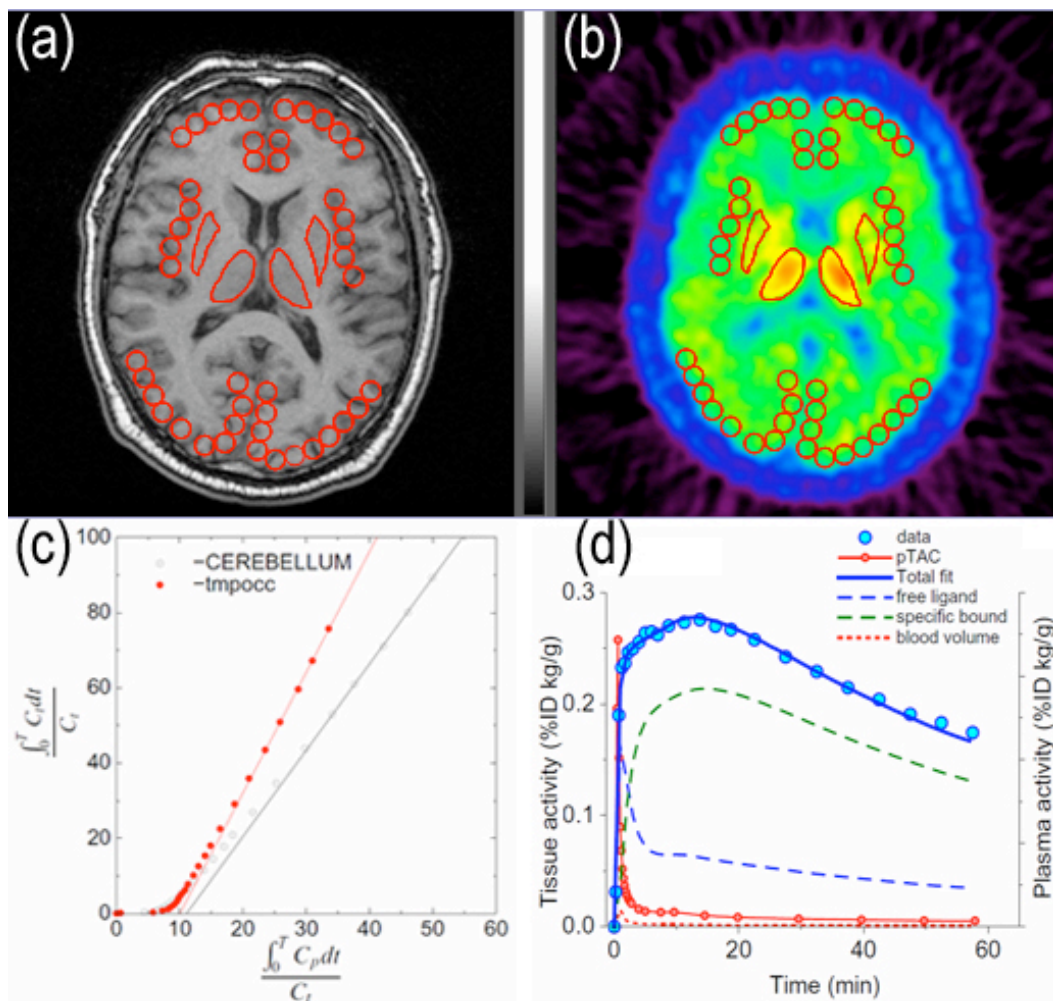


Figure 1. Regions of interest (ROIs) defined in the cerebral cortex and subcortical deep nuclei in the MRI (a) and the co-registered PET image taken from a healthy volunteer subject (b); result of linearization using Logan graphical analysis (c); and time activity curves in plasma and brain tissue for compartmental model analysis (d) are demonstrated.

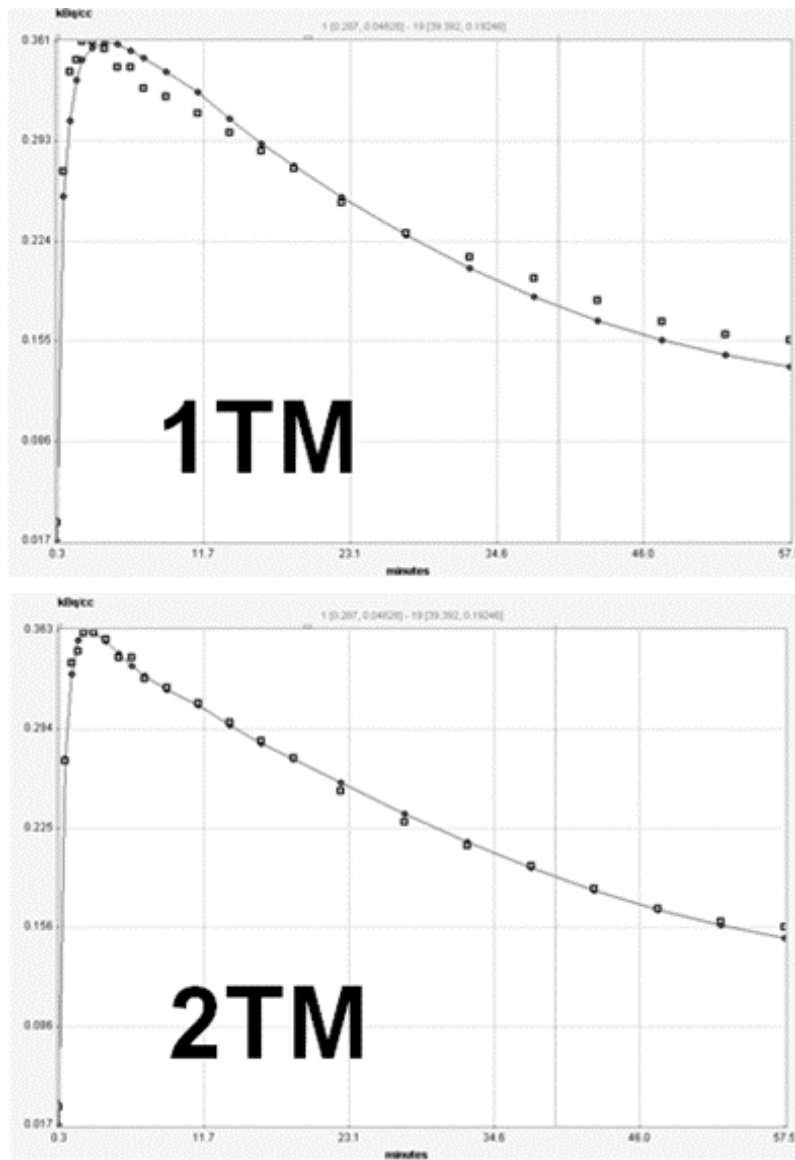


Figure 2. Results of fitting for the time activity curve in the temporoparietal cortex of an Alzheimer's disease patient based on 1-tissue (LEFT) and 2-tissue compartmental models (RIGHT). 2-tissue model gives better fitting result.